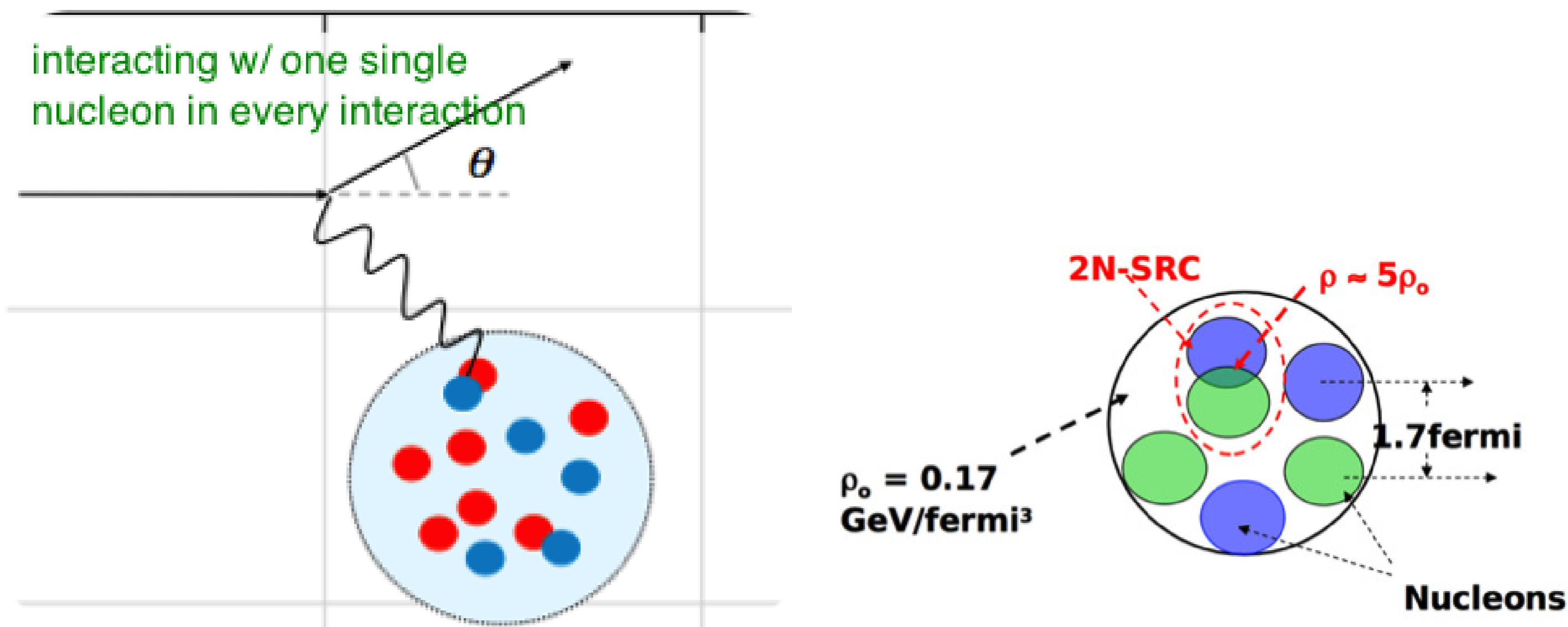


# Nuclear models: should the neutrino community care about them?

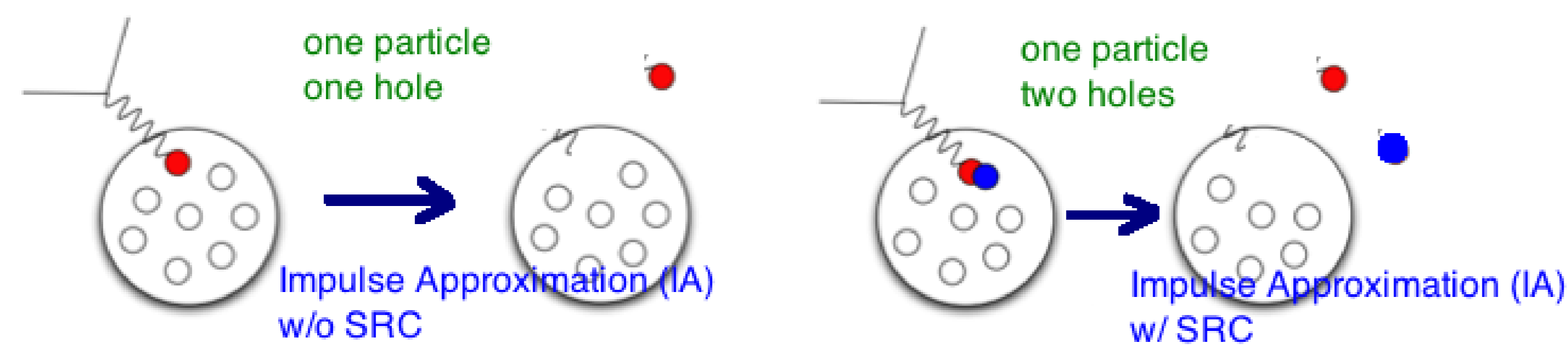
Dr. Chun-Min (Mindy) Jen

Center for Neutrino Physics, Virginia Tech, Blacksburg, VA 24061, USA

## Impulse Approximation (IA) and Short Range Correlation



## One Particle One (Two) Hole (IA Scheme)



## Spectral Function

The initial-state of the target nucleus is described by the spectral function in Eq. 1,  $P(|\vec{p}|, E)$ , yielding the probability of removing a nucleon of momentum  $\vec{p}$  from the target nucleus, leaving the residual system with the excitation energy  $E$ .

$$P(|\vec{p}|, E) = \langle \Phi_A | \Phi_{A-1}, p \rangle |\delta(E_A - E_{A-1} - m - \epsilon_0 + E)| \quad (1)$$

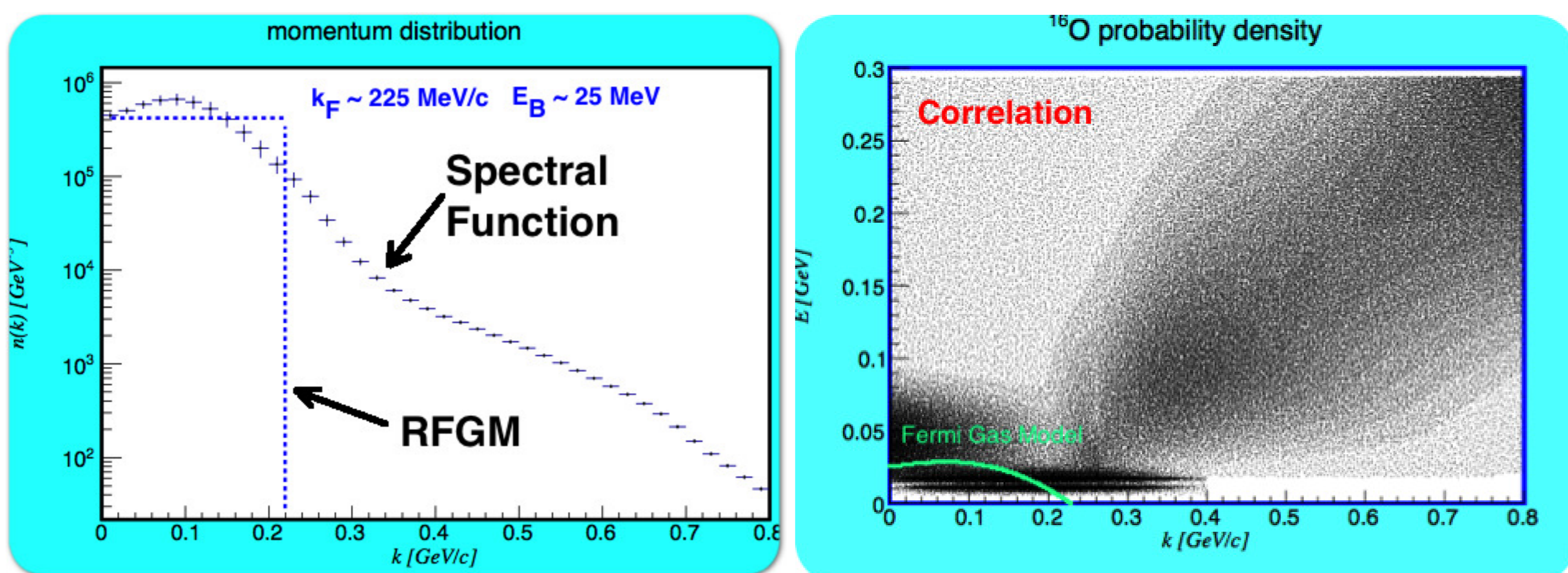


Figure 3: initial-state momentum distribution of structured nucleons (left), correlation between momentum and separation (binding) energy (right).

Within the RFGM, the spectral function is parametrized in the simple form

$$P(|\vec{p}|, E) = \frac{3}{4\pi p_F^3} \theta(p_F - |\vec{p}|) \delta(\sqrt{|\vec{p}|^2 + m^2} - m - \epsilon_0 + E) \quad (2)$$

where  $p_F \sim 250$  MeV and  $\epsilon_0 \sim 25$  MeV are the Fermi momentum and the average nucleon binding energy, respectively, and the distribution of Fig. ?? collapses to a line.

## $Q^2$ Selection at the Interaction Vertex

In GENIE 2.8.0,  $Q^2$  is selected randomly within a range defined by a set of minimum and maximal values. Therefore, the value of  $Q^2$  is not affected by the initial nucleon's kinematics, dictated by the dynamical model employed to describe the target ground state: RFGM or SF. In our implementation, the  $Q^2$  selection instead takes into account the dependence of the interaction vertex on both separation energy and initial-state momentum of the struck nucleon.

$$\left( \frac{d^2\sigma}{d\omega d\Omega_{k'}} \right)_N \propto L_{\mu\nu}(k, k') W^{\mu\nu}(\vec{p}, \vec{p} + \vec{q}), \quad (3)$$

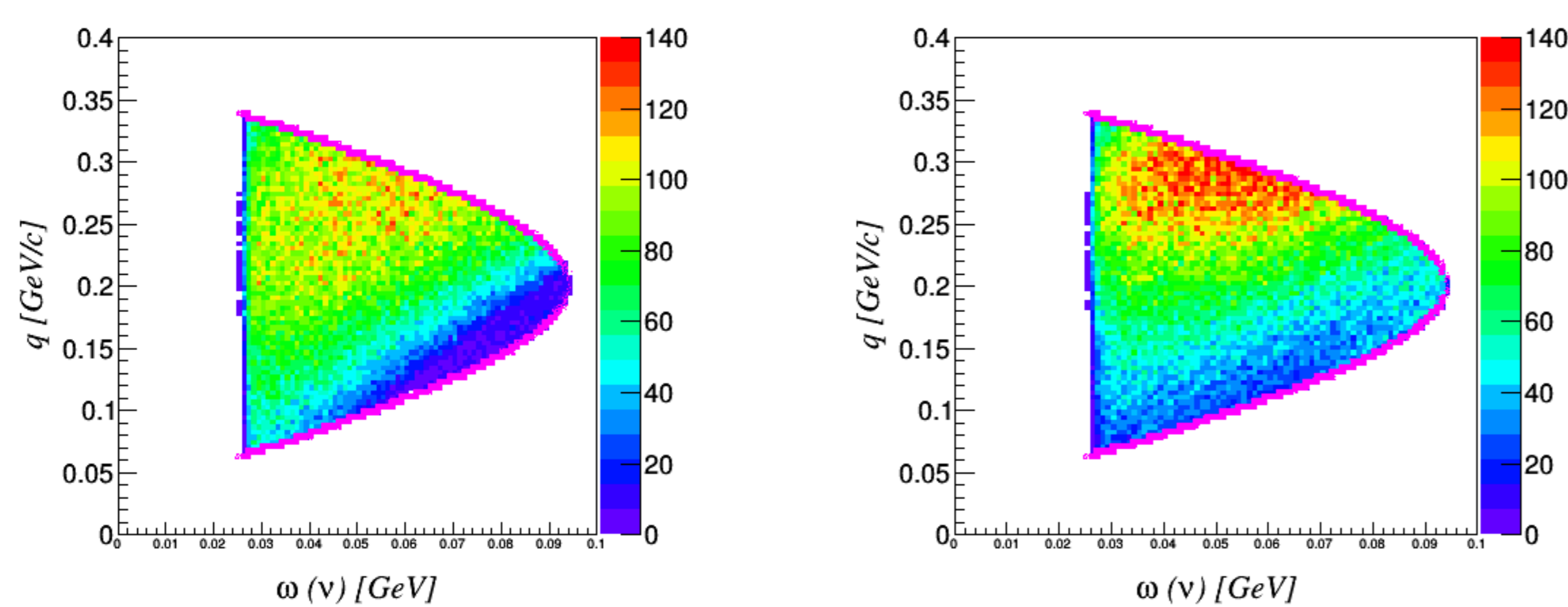


Figure 4: ( $|q|$ ,  $\omega$ ) at  $E_\nu = 200$  MeV, GENIE 2.8.0 +  $\nu T$  with RFGM (left) and SF (right).

## Cross-section

The derivation of the double differential nuclear cross section in the impulse approximation regime is described in detail in Refs. [1, 2].

$$\left( \frac{d^2\sigma}{d\omega d\Omega_{k'}} \right)_A = \int dp dE \left( \frac{d^2\sigma}{d\omega d\Omega_{k'}} \right)_N \times p^2 P(|\vec{p}|, E) \times \delta(\omega + M_A - \sqrt{|\vec{p} + \vec{q}|^2 + m^2} - E_{A-1}), \quad (4)$$

where  $p^2 P(|\vec{p}|, E)$  reflects the probability of interacting with the structured nucleon at its binding energy and initial-state momentum, and thus manifests the contribution of the lepton-nucleon interaction to the cross-section.

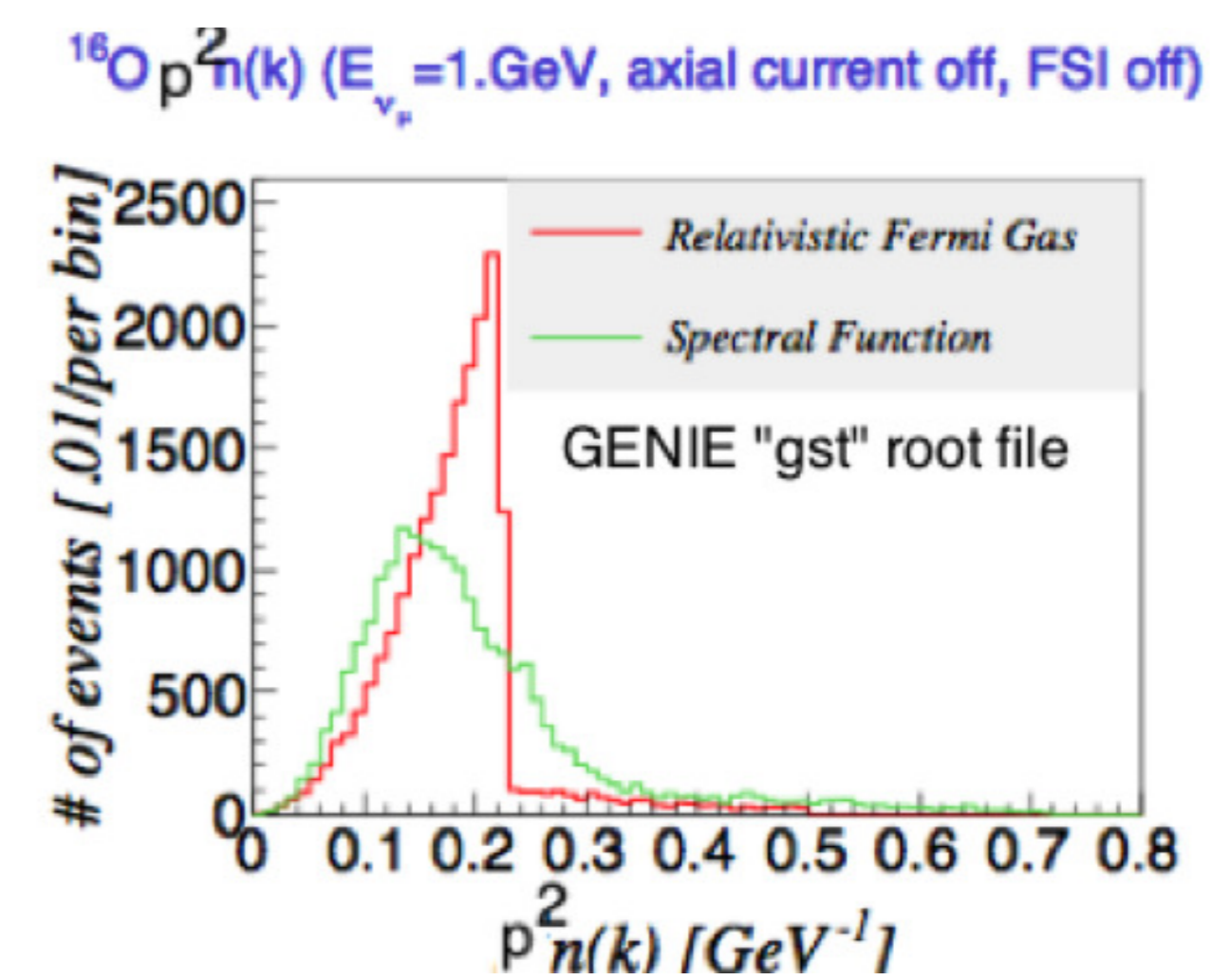


Figure 5: probability distribution of nucleon momentum  $p^2 P(|\vec{p}|, E)$ .

## Validation of Electron Cross-section

Comparison of double differential electron-nucleus cross sections between experimental data and simulated predictions in the quasi-elastic channel are shown below:

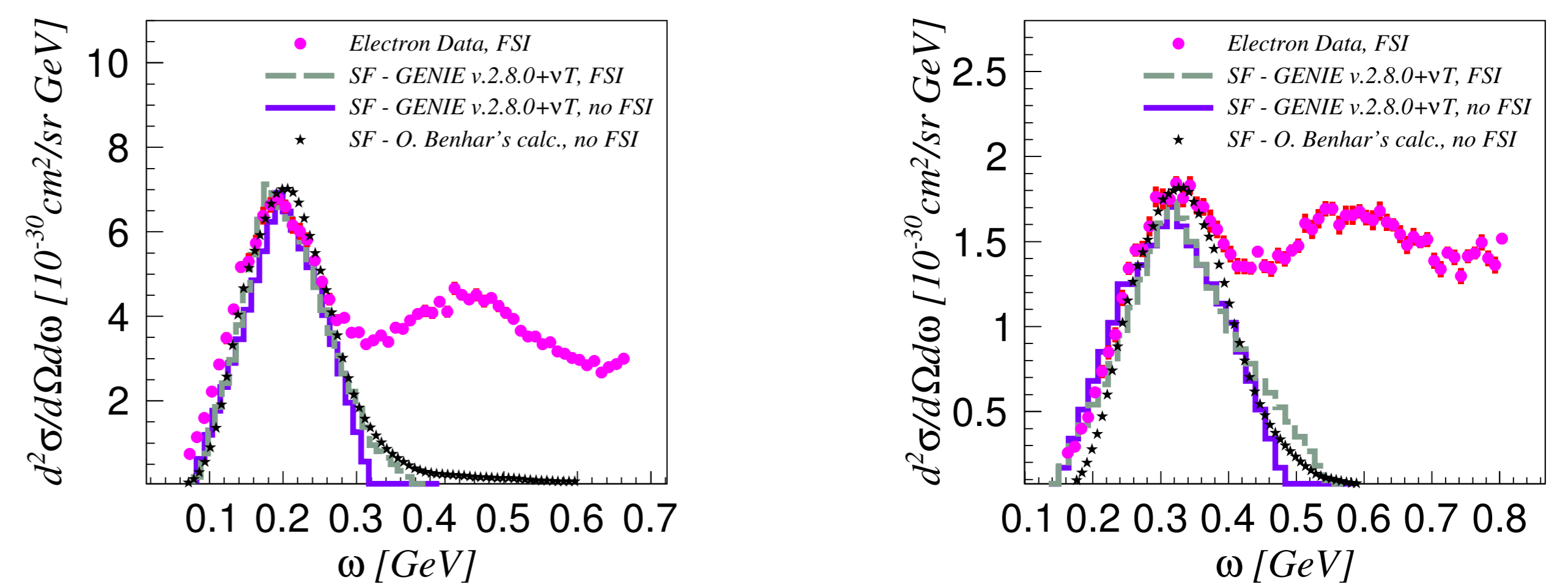


Figure 6:  $e + C \rightarrow e' + X$ ,  $E_e = 0.961$  GeV (left) and  $1.299$  GeV (right),  $\theta_e = 37.5$  deg.

## Neutrino Cross-section

Comparison of the differential CCQE  $d\sigma/dE_\mu$  cross sections of (a) oxygen and (b) argon at neutrino energy  $E_\nu = 800$  MeV, obtained using GENIE 2.8.0 +  $\nu T$  with RFGM and SF.

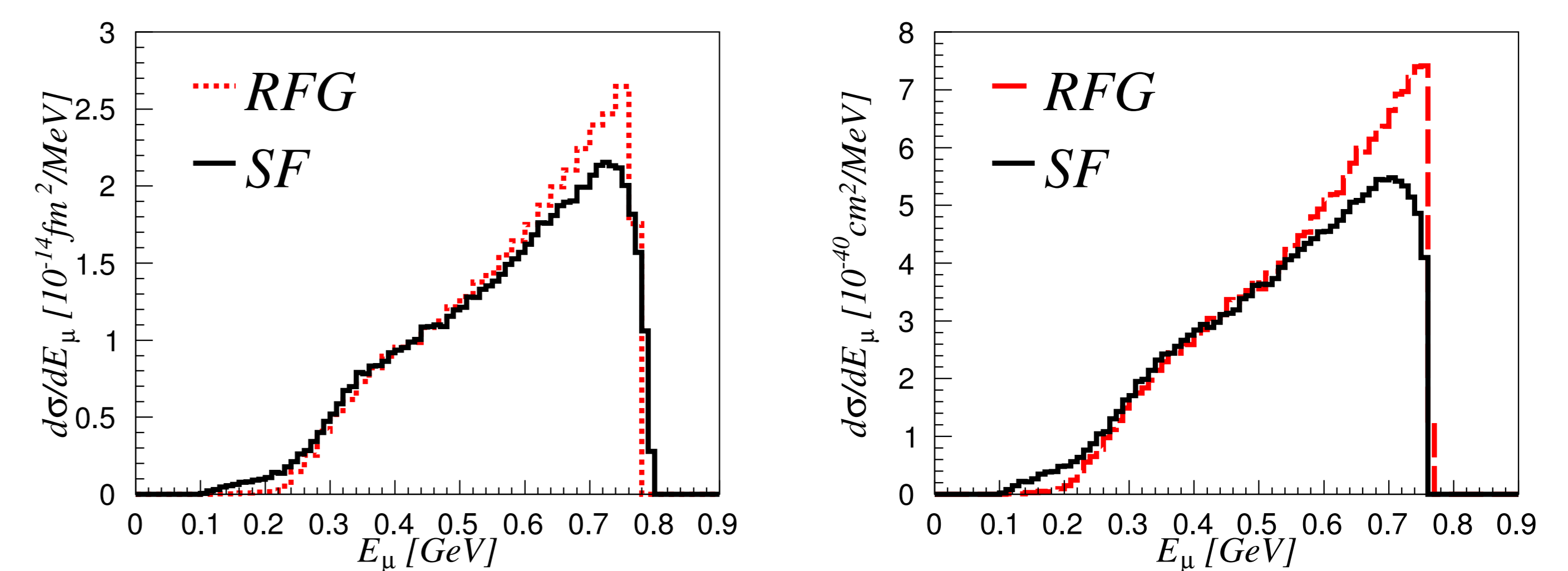


Figure 7:  $\nu + O \rightarrow \mu + X$ , no Pauli blocking, no FSI (left),  $\nu + Ar \rightarrow \mu + X$  (an approximation of  $^{40}Ca$ ), Pauli blocking and FSI included (right).

## Neutrino Oscillation Parameters

To evaluate the impact of three different simulation conditions (RFGM, RFGM + new  $Q^2$  selection and SF) we took the event rates computed using GLOBES, applied to them the migration matrices computed with one particular setting of the neutrino interaction generator, and try to fit them using the matrices obtained with a different setting. By doing this, the possible biases on the oscillation parameters, induced by the different nuclear models or  $Q^2$  selection introduced in GENIE 2.8.0 +  $\nu T$ , can be quantified in a robust fashion.

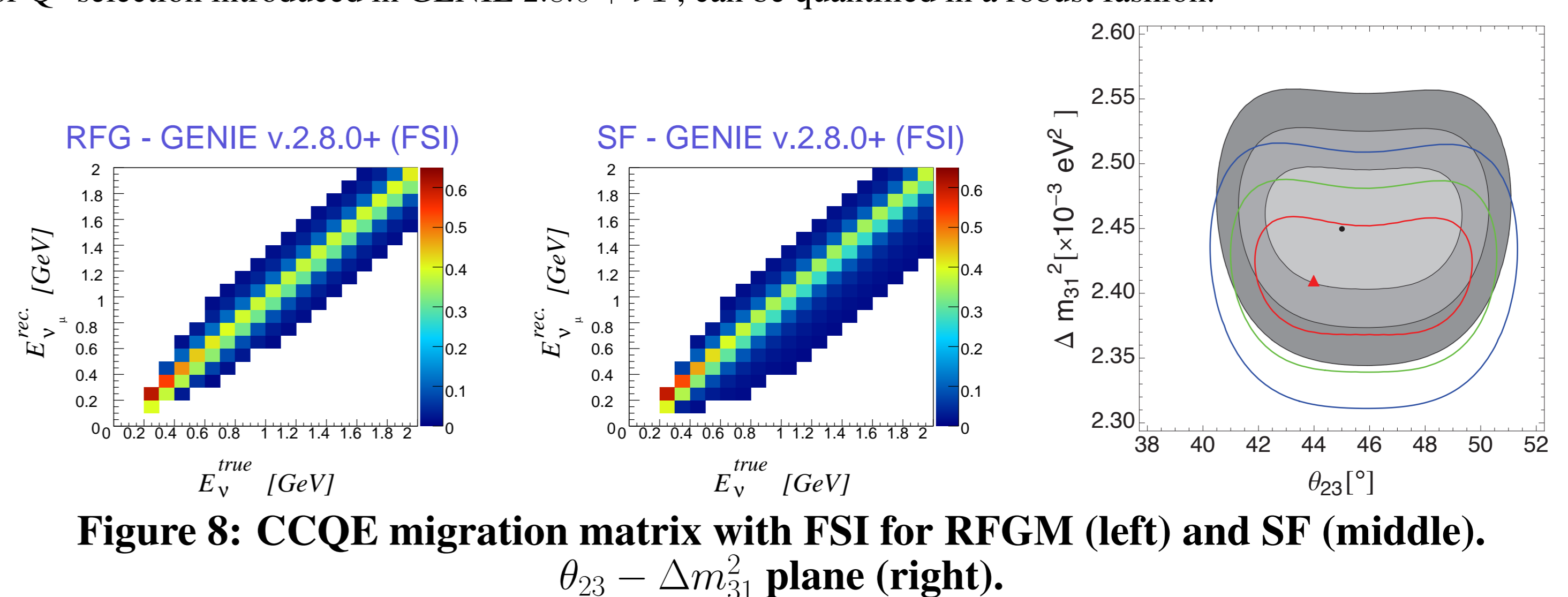


Figure 8: CCQE migration matrix with FSI for RFGM (left) and SF (middle),  $\theta_{23} - \Delta m_{31}^2$  plane (right).

The shaded area shows the confidence regions that would be obtained at 1, 2 and  $3\sigma$  if the simulated and fitted event rates are generated using the same set of migration matrices produced by GENIE 2.8.0 +  $\nu T$  and SF. The colored lines show the resulting regions if the event rates are computed using matrices produced by GENIE 2.8.0 +  $\nu T$  and RFGM are fitted with the rates computed using matrices obtained using GENIE 2.8.0 +  $\nu T$  and SF. The red dot shows the true input value of the fit, while the red triangle shows the location of the best fit point.

## Acknowledgement

Artur Ankowski, Omar Benhar, Andrew Furmanski, Donal Day, Steve Dytman, Douglas Higinbotham, and Camillo Marani.

## References

- [1] Benhar, Omar and Farina, Nicola and Nakamura, Hiroki and Sakuda, Makoto and Seki, Ryoichi, *Phys. Rev. D* **72**, 053005 (2005).
- [2] Benhar, Omar and Day, Donal and Sick, Ingo, *Rev. Mod. Phys.*, **80**, 189 (2008)